Journal of Physics: Conference Series **125** (2008) 012027 doi:10.1088/1742-6596/125/1/012027

Interaction of turblence and chemistry in a low-swirl burner

J B Bell[1], R K Cheng[2], M S Day[1], V E Beckner[1] and M J Lijewski[1]

[1]Center for Computational Science and Engineering, Lawrence Berkeley National Laboratory, Berkeley, CA, 94720, USA

[2]Environmental Energy Technologies Division, Lawrence Berkeley National Laboratory, Berkeley, CA, 94720, USA

E-mail: jbbell@lbl.gov

Abstract. New combustion systems based on ultra-lean premixed combustion have the potential for dramatically reducing pollutant emissions in transportation systems, heat, and stationary power generation. However, lean premixed flames are highly susceptible to fluid-dynamical combustion instabilities, making robust and reliable systems difficult to design. Low-swirl burners are emerging as an important technology for meeting design requirements in terms of both reliability and emissions for next-generation combustion devices. In this paper, we present simlations of a laboratory-scale low-swirl burner using detailed chemistry and transport without incorporating explicit models for turbulence or turbulence/chemistry interaction. We consider two fuels, methane and hydrogen, each at two turbulent intensities. Here we examine some of the basic properties of the flow field and the flame structure. We focus on the differences in flame behavior for the two fuels, particularly on the hydrogen flame, which burns with a cellular structures.

1. Introduction

Low-swirl burner technology was introduced by Bedat and Cheng [1] as tool for studying the fundamental properties of lean, premixed turbulent flames. Burners based on modifications of the original design have been used by a number of research groups [2–5] and have the potential for use in the design of next-generation, lean premixed combustion systems, including those burning lean hydrogen mixtures, both at atmospheric and elevated pressures [6].

The low-swirl burner concept is extremely simple: premixed fuel (here, lean hydrogen or methane mixtures) exits a pipe with circular cross section (5-10 cm in radius) after passing through a turbulence plate and an annular set of curved vanes. The vanes impart a swirl component to the flow over a narrow layer near the pipe wall. The flow then diverges radially at the pipe exit, and a detached premixed flame propagates freely in the flow field. The turbulence is introduced into the fuel stream to produce wrinkles in the flame and enhances the overall rate of combustion in the device; the flames stabilize where the mean burning speed matches the axial flow velocity. Analysis of experimental velocity measurements for both lean hydrogen-air and methane-air mixtures shows that the mean burning speed of the low-swirl flames is proportional to the intensity of turbulence in the approach flow to the flame [6, 7], and that effective enhancement of the burning speed can exceed a factor of 50 or more. However,

because the burner supports ultra-lean mixtures while also lacking a significant postflame flow recirculation, nitrogen-based emissions are extremely low.

Continued development of these types of burners, particularly for practical combustion devices, depends on improving our understanding of basic flame structure, stabilization mechanisms, emissions, and response to changes in fuel. Numerical modeling has the potential to address some of these issues; however, simulation of these types of burners has proven to be difficult because of the large range of spatial and temporal scales in the system; the bulk of the analysis to date has been experimental. The work of Nogenmyr et al. [4], which simulated low-swirl methane flame using LES with a G-equation formulation, was one of the first successful simulations of these types of flames.

The basic issues for these flames become particularly important, and difficult to simulate, for certain advanced fuels. Lean hydrogen-air flames burn in cellular structures—localized regions of intense burning, separated by regions of local extinction. Such a discontinuous flame surface introduces severe difficulties in applying standard turbulence/chemistry interaction models, which are based on the presence of a highly wrinkled but continuous flame surface that propagates locally as an idealized laminar flame structure. The cellular burning patterns additionally make the analysis of experimental data problematic and can lead to significant inaccuracies or misinterpretations.

We consider an alternative approach to the study of these flames based on detailed numerical simulations carried out at the laboratory scale without including turbulence models. Our target low-swirl burner configuration, presented in [2], is under investigation by several groups internationally using matched nozzle hardware and is designed specifically to support validations with computer simulation.

2. Numerical methodology

The simulations presented here are based on a low Mach number formulation [8] of the reacting Navier-Stokes equations that offers a significant performance benefit for these types of turbulent flame simulations [9]. The methodology treats the fluid as a mixture of perfect gases. We use a mixture-averaged model for differential species diffusion, which is critical to capturing the thermodiffusive behavior of lean hydrogen flames (see [10] for a complete discussion of this approximation). We ignore Soret, Dufour, and radiative transport processes. The transport coefficients, thermodynamic relationships, and chemical source terms are obtained from a CHEMKIN-compatible specification. The methane flame with inlet mixture, $\phi = 0.7$, was modeled with DRM-19; the hydrogen flame, $\phi = 0.37$, was based on the hydrogen sub-mechanism of GRI-Mech 2.11. The basic discretization [11] combines a symmetric operator-split treatment of chemistry and transport with a density-weighted approximate projection method to impose the evolution constraint. The resulting integration proceeds on the time scale of the relatively slow advective transport. Faster diffusion and chemistry processes are treated implicitly in time. This integration scheme is embedded in an adaptive mesh refinement algorithm based on a hierarchical system of rectangular grid patches. The data and work are apportioned over a parallel computing system using a coarse-grained load distribution strategy [12]. The complete integration algorithm is second-order accurate in space and time and discretely conserves species mass and enthalpy.

3. Computational setup

We use an experimental characterization of the flow at the nozzle exit to generate a suitable inflow boundary condition for the simulations. Typical profiles for this purpose were provided by Petersson et al. [2] and are shown in figure 1 as a function of radius from the centerline of the fuel pipe. Outside the pipe, a 35 cm/s upward coflow is specified. Turbulent fluctuations in the nozzle were prepared in an auxiliary simulation and added to the mean flows. An initially zero-mean

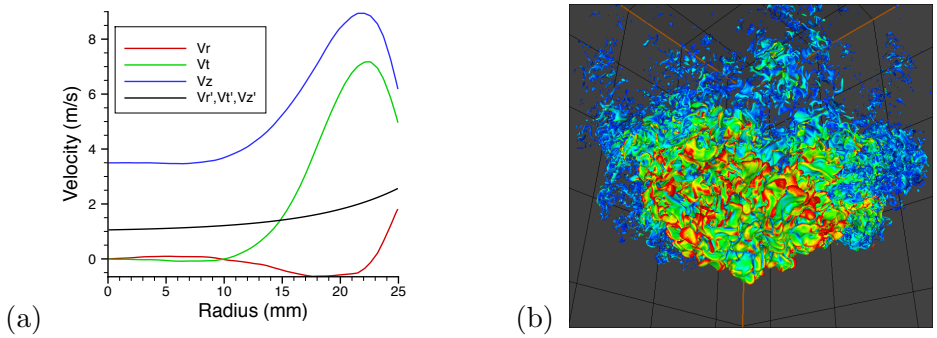

Figure 1: (a) Inlet velocity profiles at the exit plane of the swirl nozzle, adapted from experimental data [2]. (b) Instantaneous snapshot of typical H_2-air flame burning in 3D cellular structures (view angle is looking up from below the exit plane of the nozzle, radius = 25 mm). An isotherm in the flame zone is shown and is colored by the local rate of fuel consumption–the red areas are burning intensely, the blue areas are extinguished.

velocity field, representative of flow through a perforated plate, is evolved until the measured integral length scale was 4 mm, and the fluctuation intensity matched the value measured at the device core. A radial scaling factor was used to shape these synthetic fluctuations to the measured data. For the second, "high-turbulence" case, we simply scaled all inlet profiles at the nozzle by 250%.

The thermal thicknesses of these flames are approximately 600–800 μm; the full half-width maximum of the fuel consumption rate is 250–500 μm. The computational domain for the reacting flow simulations measures $(25\text{cm})^3$. We implicitly assume that the boundaries of this box are sufficiently far from the flame as to not significantly affect its dynamics. The base mesh for the simulation is a uniform grid of 256^3 cells and uses three additional levels of factor-of-two dynamic grid refinement that track regions of high vorticity (turbulence) and reactivity (combustion/flame). In all cases, the flame is contained entirely within the finest level, for an effective resolution of 2048^3. We run the simulations from an arbitrary initial condition until the flame is statistically stabilized without the finest level of resolution. Prior to collecting data for analysis, we add the finest level of resolution and continue the numerical integration until the flame statistics cease to vary in time. At the finest resolution of these computations, our simulation methodology resolves the detailed structure of both the methane and hydrogen flames—the time-dependent location of the peak fuel consumption, the thermal field and major species are numerically converged, and the profiles of most of the flame radicals are well-represented.

4. Simulation results

A typical snapshot of the high-turbulence with lean hydrogen is shown in figure 1(b). The image is of an isotherm in the flame zone (T=1139 K), colored by the local consumption rate of fuel. The red regions indicate burning at up to 16 times the flat laminar flame value. The blue regions indicate local extinction and separate the cellular burning structures in this thermodiffusively unstable flame. In figure 2 we show fuel and OH in a slice through the center of the burner for all four cases. The solution was advanced at both resolutions for 50 coarse time steps after the final level of refinement was added prior to making comparisons. This corresponds to 200 time steps at 244μm and 400 time steps at 122μm. The images demonstrate that the methodology is capable of resolving the overall flame shape as well as the chemical detail of the flame. Similar grid-independence is observed for the other state quantities.

The methane flame shows an increased wrinkling with the increased level of turbulence; however, as shown by the OH profile, combustion along the flame front is relatively insensitive

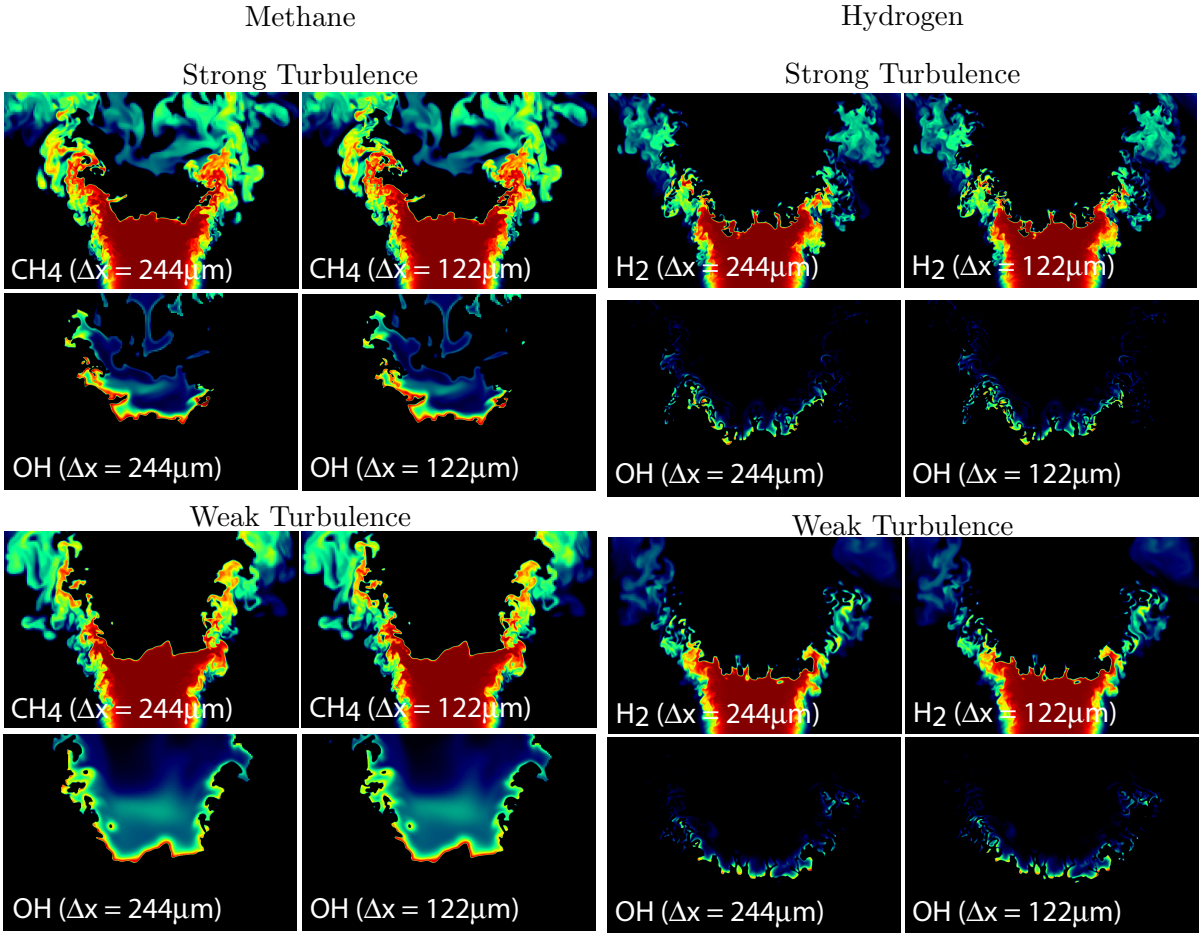

Figure 2: Fuel and OH mole fraction normalized to the peak value in the flat flame, for the four simulations cases. Snapshots taken on slices through centerline of domain indicate robust grid-independent solutions.

to stretch effects as expected for methane flames at $\phi = 0.7$. The high diffusivity of H_2 makes the hydrogen flame at $\phi = 0.37$ thermodiffusively unstable so that it burns with a cellular structure. As a consequence of this cellular burning the wrinkling of the hydrogen flame is considerably more pronounced. Examination of the OH images shows the cellular structure more clearly. The flame front is broken with regions of intense burning separated by regions of local extinction. As in the methane case, increasing turbulence leads to an increase in the wrinkling of the flame and a reduction in the overall size of the features along the flame front.

We next consider the effect of the fuel on the overall turbulent burning rate. In all the flames computed, there is a qualitatively different interaction between the flame and the vortical structures due to the inlet turbulence, and those due to the the breakdown of the mean swirling flow. For that reason, we restrict our consideration to the central core region of the burner. We can estimate the burning speed in this core region by integrating the instantaneous fuel consumption rate over a cylindrical volume with the same radius as the nozzle up to a height of 10 cm. This regions captures all of the core burning. We then normalize this integral by $\rho Y_{F,in} \times A_{in} \times s_L$ where A_{in} is the inflow area of the burner, $\rho Y_{F,in}$ is inflow fuel density and s_L is the laminar flame speed. The resulting data for the four cases are presented in figure 3. (We note that this measure does not represent a traditional definition of the turbulent flame speed. For that type of measurement, we would need the predict the flame brush to correctly normalize the integrals. Here, we do not have sufficient data for that prediction.

Our definition, in effect, assumes that the flame brush is flat.) This figure shows several interesting features. First, the turbulent flame speed enhancement for the hydrogen flame is much larger than for the methane flame. In addition, the response to increasing the level of turbulence is stronger for the hydrogen flame. These characteristics are a result of the thermodiffusive instability of the hdyrogen flame. In addition, we note that extrapolation to zero turbulence gives the laminar flame speed for methane but shows an enhanced speed for hydrogen. This is again because of the thermodiffusive instability; even in the absence of turbulence, the hydrogen flame will burn with a cellular structure at an enhanced flame speed, see [13].

We have presented simulations of an experimental low swirl burner with detailed chemistry and transport without introducing any turbulence models. The simulations demonstrate the level of resolution needed to accurately characterize the flames and shows that the methodology can capture the cellular structure of the hydrogen flame. In future work, we will provide a more detailed analysis of the simulation results focusing on local flame properties and comparison with experimental results. In future simulations, we plan to include nitrogen emissions chemistry to explore the formation of NO_x and to investigate the structure of these types of flames at higher pressures.

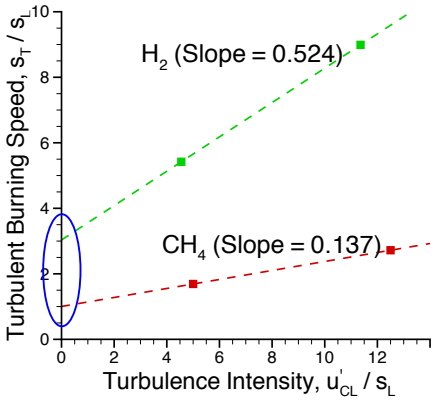

Figure 3: Computed turbulent burning speeds in the central core of the burner.

Acknowledgments

This work was supported by the SciDAC Program of the DOE Office of Mathematics, Information, and Computational Sciences under the U.S. Department of Energy under contract No. DE-AC02-05CH11231. The computations presented here were performed on Franklin, the XT4 at NERSC as part of an INCITE award. The authors thank A. Dreizler and P. Petersson for providing experimental velocity measurements used to define the boundary conditions.

References

[1] Bedat B and Cheng R K 1995 *Combust. Flame* **100** 485–494
[2] Peterson P, Olofsson J, Brackman C, Seyfried H, Zetterberg J, Richter M, Alden M, Linne M, Cheng R, Nauert A, Geyer D and Dreizler A 2007 *Appl. Opt* **46** 3928–3936
[3] Cheng R K 1991 *Combust. Flame* **101** 1–14
[4] Nogenmyr K, Peterson P, Bai X, Nauert A, Olofsson J, Brackman C, Seyfried H, Zetterberg J Li Z S, Richter M, Dreizler A, Linne M and Alden 2007 *Proc. Combust. Inst* **31** 1467–1475 *submitted to LACSEA Feature Issue*
[5] Mansour M and Chen Y C 2007 *Experimental Thermal Fluid Sci. in press*
[6] Cheng R K, Littlejohn D, Strakey P A and Sidwell T 2008 *Proc. Combust. Inst.* 21–46 to appear
[7] Cheng R K and Littlejohn D 2008 *Proceedings of GT2008: ASME Turbo Expo 2008* (Berlin, Germany: ASME) paper GT2008-50504
[8] Rehm R G and Baum H R 1978 *N. B. S. J. Res.* **83** 297–308
[9] Bell J B, Aspden A J, Day M S and Lijewski M J 2007 *Numerical Simulation of Low Mach Number Reacting Flows* (*Journal of Physics Conference Series: SciDAC 2007 (W. Tang, Ed.)* vol 78) (Boston, Massachusettes: Institute of Physics Publishing) p 012004
[10] Ern A and Giovangigli V 1994 *Multicomponent Transport Algorithms* (*Lecture Notes in Physics* vol m24) (Berlin: Springer-Verlag)
[11] Day M S and Bell J B 2000 *Combust. Theory Modelling* **4** 535–556
[12] Rendleman C A, Beckner V E, Lijewski M, Crutchfield W Y and Bell J B 2000 *Computing and Visualization in Science* **3** 147–157
[13] Day M S, Bell J B, Bremer P T, Pascucci V and Beckner V E In preparation